

MINERALOGY AND GEOCHEMISTRY OF LUNAR MAGNESIAN BRECCIA DHOFAR 1085

X. H. Fu^{1,2}, X. T. Hou¹, H. J. Cao¹, J. Chen¹, Z. C. Ling¹. ¹ Shandong Provincial Key Laboratory of Optical Astronomy and Solar-Terrestrial Environment, Institute of Space Sciences, Shandong University (fuXH@sdu.edu.cn). ²Key Laboratory of Lunar and Deep Space Exploration, National Astronomical Observatories, Chinese Academy of Sciences.

Introduction: Lunar samples preserve a great record of the geological evolution of the Moon. Laboratory investigations of Apollo and Luna samples provide the key to understand the Moon's origin and geological evolution. However, all Apollo missions landed near to or within the Procellarum KREEP Terrane (PKT) [1,2]. This may bias and limit our understanding of the global Moon. Lunar meteorites are another important source of materials from the Moon, which are randomly ejected from lunar surface. They have greatly increase the diversity of highland materials beyond those collected by Apollo and Luna missions, and present challenges to the Lunar Magma Ocean (LMO) theory [3-7]. Dhofar 1085 is a lunar meteorite found in Oman. It is an impact melt breccia consisting of mineral fragments and lithic clasts, paired with Dhofar 489 clan [8-10]. This study investigated the petrographic and mineralogical characteristics of a meteorite sample Dhofar 1085, and determines its major lithic types, mineral chemistry, impact metamorphism and weathering degree.

Sample and experimental methods: The petrography study was performed on one thin section of Dhofar 1085 using a Leica DM2700 P Microsystems. Back-scattered Electron (BSE) images of Dhofar 1085 thin section were obtained with a FEI Nova NanoSEM 450 in Shandong University, Weihai, China. Chemical composition of minerals were determined using an Oxford INCA EDS (X-Max50) with an ultrathin windowed Si (Li) detector. Raman spectra of Dhofar 1085 were measured by Renishaw inVia® Raman Microscope in Shandong University. We employed a green laser (532 nm) for excitation and measured Raman shift range of 100~2000 cm^{-1} with a spectral resolution better than 1 cm^{-1} . Before each measurement, a Si wafer was used as the wavelength calibration standard. The 100 \times objectives were used for the fine-grained phase analysis and the spatial resolution of laser spot is better than 1 μm .

Petrography and Mineralogy: The meteorite Dhofar 1085 has a typical breccia texture with a fine-grained, well-crystallized impact-melt matrix (Figure 1). The rock fragments are all highland rock types. The dominant lithic clast are anorthosite with granulitic texture. The plagioclase grains are up to 4 mm and partially transformed to maskelynite due to impact shock. The fine-grained mafic minerals (20-50 μm) are embedded in large subrounded plagioclase grains. The second group of lithic clasts are coarse-grain granulite,

which are characterized with abundant mafic minerals with relative large grain size (0.5-1.0 mm). The largest one of this group is a troctolitic anorthosite (up to 4 mm in size), which contains an aggregate of rounded olivine grains (Fo_{80-91} , Figure 2). This clast is texturally consistent with the spinel troctolite clast in Dhofar 489 [8]. However, in this clast and even the whole meteorite, we found no Mg-Al spinel. Mare basalt, KREEP-related materials, and even granitic materials were reported in Dhofar 489 and other paired rocks [6], which are also absent in this meteorite.

The matrix of Dhofar 1085 consists of single mineral fragments up to 4 mm in size. The majority of mineral fragments are plagioclase and olivine. The largest olivine grain (Fo_{80}) is up to 1.5 mm (Figure 2). The other mafic mineral pyroxene is relatively rare in Dhofar 1085. Accessory phases, including chromite, FeS, FeNi metal, are identified in this rock.

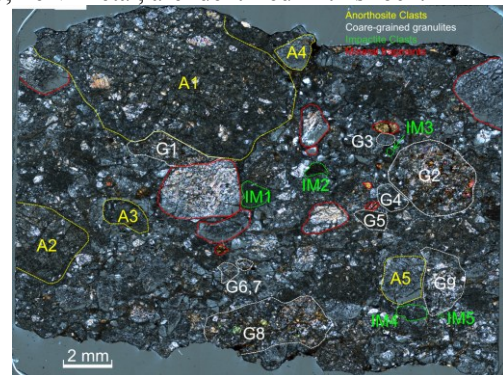


Figure 1 The cross polarized light image of Dhofar 1085. The yellow, white, green lines represent anorthosite (A1-5), coarse-grain granulite clasts (G1-9) and recrystallized impact melts (IM1-5). The red lines indicate olivine, pyroxene and plagioclase fragments.

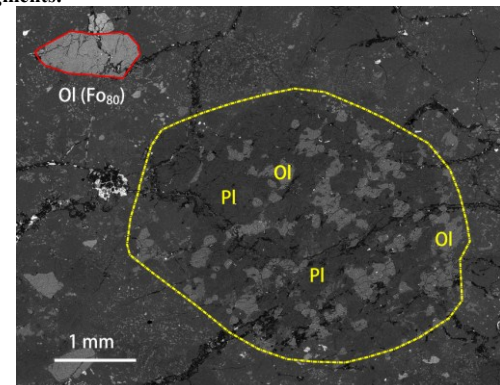


Figure 2 BSE image of coarse-grain granulite (G2 in Figure 1). The top-left phase is a large relict olivine grains.

We determined the Fo value of olivine and the En and Wo values of lunar pyroxene using their Raman peak positions following the methods in [11,12]. Figure 3 shows the composition of mafic minerals in Dhofar 1085. The clasts in this rock bridged the gap between the Mg suite and ferroan anorthosite suite (FAN) from Apollo samples (Figure 3). This indicates this meteorite is a breccia composed of magnesian anorthositic lithologies.

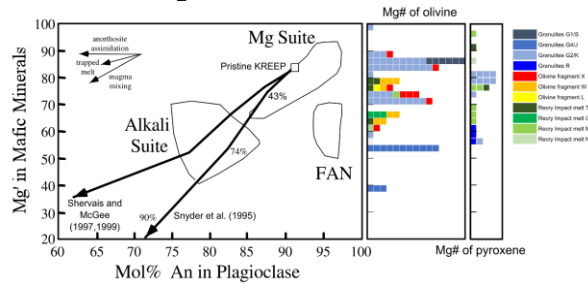


Figure 3 The olivine and pyroxene compositions in the lithic clasts of Dhofar 1085. The diagram is modified from the reference [13].

Bulk chemistry: Korotev et al. (2012) analyzed the bulk compositions of four Dhofar 1085 chips using INAA method [10]. The average FeO concentration of this meteorite is 3.18 wt%, which is lower than most lunar anorthositic meteorites (2.9-7.0 wt%). The Cr/Sc ratio could be used a proxy for the Mg/Fe ratio [2]. The Cr/Sc ratio (118-147) of Dhofar 1085 are higher than those of typical FANs (60-105) and mare basalts (40-110). This suggest this meteorite is chemically primitive.

The Sc concentration of this meteorite (3.92-4.63 ppm) are lower than other meteorites ALH 81005 and NWA 2995 containing magnesian anorthositic granulites (MAN) [7]. This chemical feature agrees with the scarcity of pyroxene concluded from the petrographic observation.

Dhofar 1085 shares the similar REE patterns with the paired rock Dhofar 489 [8]: low abundance of REE, LREE relative rich ($La/Yb=14.3$), Eu positive anomaly. The REE abundance of Dhofar 1085 and other paired rocks locate between typical FANs and Mg-suite. The Th concentration (0.05-0.07 ppm) is also the lowest among brecciated lunar meteorites.

Source region of Dhofar 1085: Takeda et al. (2006) suggest that Dhofar 489 is from lunar farside on the basis of the feldspathic composition and low concentration of Th and other incompatible elements (ITE) in the meteorite. Korotev et al. (2006) concluded that this meteorite is most likely to originate from the northern feldspathic highlands, some of which lie on the nearside. Dhofar 1085's low FeO and ITEs chemistry suggests it most likely came from the highlands, being far away from PKT and mare regions.

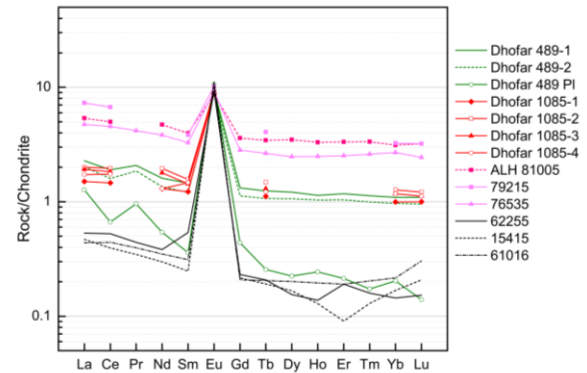


Figure 4 CI-chondrite normalized REE patterns for Dhofar 1085 bulk samples. Lunar samples 62255, 15415, and 61016 are typical FAN and 79215 and 76535 are Mg-rich suite. Apollo samples data are from the reference [14]. Data of Dhofar 489 and ALH 81005 are from the references [8] and [15].

Shock effects and terrestrial weathering: Under the polarized microscopy, the impact plane foliation (PDF) are observed in some plagioclase grain or their rims in Dhofar 1085. Broad and weak Raman peaks of these plagioclase indicate that these phases transformed into maskelynite. We suggest that the impact metamorphism of this meteorite is S4. Terrestrial alterations, including Fe oxide/hydroxides, gypsum, and barite, have been identified in the cracks. The weathering degree of the rock can be determined as W3 by microscopic observation.

Future works: Our future works include measuring major and trace elements in individual minerals using electron probe and LA-ICP-MS. Using these data, we will better constrain its origin and potential relationship to Apollo Mg-suite or FAN lithologies.

Acknowledgments: This work is supported by the grant from Key Laboratory of Lunar and Deep Space Exploration, CAS and the opening fund of State Key Laboratory of Lunar and Planetary Sciences (Macau University of Science and Technology) (Macau FDCT grant No. 119/2017/A3).

References: [1] Warren et al. (2005) *MAPS*, 40(7): 989-1014. [2] Jolliff et al. (2000) *JGR*, 105, E2, 4197-4197-4216. [3] Korotev et al. (2003) *GCA*, 67, 4895-4923. [4] Korotev et al. (2006) *Chemie der Erde*, 65, 297-346. [5] Day et al. (2006) *GCA*, 70, 5957-5989. [6] Joy and Arai (2013) *Astronomy & Geophysics*, 54, 4.28-4.32. [7] Gross et al. (2014) *EPSL*, 388, 318-328. [8] Takeda et al. (2006) *EPSL*, 247, 171-184. [9] Korotev et al. (2006) *GCA*, 70, 5935-5956. [10] Korotev (2012) *MAPS*, 47, 1365-1402 [11] Chen et al. (2017) *LPSC*, 2277#. [12] Cao et al. (2019) *Journal of Raman Spectroscopy*, 1-15. [13] Shearer et al. (2006). *Reviews in Mineralogy and Geochemistry*, 60(1), 365-518. [14] Haxsin & Warren (1996) *Lunar chemistry*, 358-474. [15] Warren et al. (1983) *GRL*, 10, 779-782.